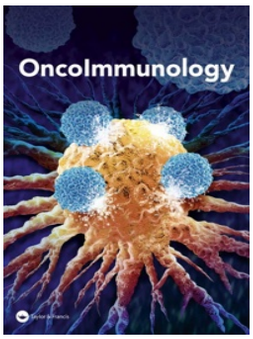

OncoImmunology

ISSN: 2162-402X (Online) Journal homepage: www.tandfonline.com/journals/koni20

Alistipes and *Eggerthella* shape the response to oncolytic adenovirus therapy in mice and humans through short-chain fatty acid metabolism

Mirte van der Heijden, James Hugo Armstrong Clubb, Pande Putu Erawijantari , Aki Ronkainen , Victor Arias, Elise Jirovec, Tatiana Kudling, Santeri Artturi Pakola, Nea Ojala , Lyna Haybout, Saru Basnet, Susanna Grönberg-Vähä-Koskela , Sini Karoliina Raatikainen , Otto Hemminki , Anna Kanerva , Dafne Carolina Alves Quixabeira, Victor Cervera-Carrascon, João Manuel dos Santos , Leo Lahti & Akseli Hemminki

To cite this article: Mirte van der Heijden, James Hugo Armstrong Clubb, Pande Putu Erawijantari , Aki Ronkainen , Victor Arias, Elise Jirovec, Tatiana Kudling, Santeri Artturi Pakola, Nea Ojala , Lyna Haybout, Saru Basnet, Susanna Grönberg-Vähä-Koskela , Sini Karoliina Raatikainen , Otto Hemminki , Anna Kanerva , Dafne Carolina Alves Quixabeira, Victor Cervera-Carrascon, João Manuel dos Santos , Leo Lahti & Akseli Hemminki (2026) *Alistipes* and *Eggerthella* shape the response to oncolytic adenovirus therapy in mice and humans through short-chain fatty acid metabolism, OncoImmunology, 15:1, 2656514, DOI: 10.1080/2162402X.2026.2656514

To link to this article: https://doi.org/10.1080/2162402X.2026.2656514

ONCOIMMUNOLOGY
2026, VOL. 15, NO. 1, 2656514
https://doi.org/10.1080/2162402X.2026.2656514

Taylor & Francis
by informa

RESEARCH ARTICLE

Alistipes and *Eggerthella* shape the response to oncolytic adenovirus therapy in mice and humans through short-chain fatty acid metabolism

Mirte van der Heijden[a], James Hugo Armstrong Clubb[a,b], Pande Putu Erawijantari[c], Aki Ronkainen[d], Victor Arias[a], Elise Jirovec[a], Tatiana Kudling[a,b], Santeri Artturi Pakola[a], Nea Ojala[a], Lyna Haybout[a,b], Saru Basnet[a], Susanna Grönberg-Vähä-Koskela[a,e], Sini Karoliina Raatikainen[b], Otto Hemminki[a,f], Anna Kanerva[a,g], Dafne Carolina Alves Quixabeira[a,b], Victor Cervera-Carrascon[a,b], João Manuel dos Santos[a,b], Leo Lahti[c] and Akseli Hemminki[a,b,e]

[a]Cancer Gene Therapy Group, Translational Immunology Research Program, University of Helsinki, Helsinki, Finland; [b]TILT Biotherapeutics, TILT Biotherapeutics Ltd, Helsinki, Finland; [c]Department of Computing, Faculty of Technology, University of Turku, Turku, Finland; [d]Green Chemistry, Metropolia University of Applied Sciences, Helsinki, Finland; [e]Comprehensive Cancer Center, Helsinki University Hospital, Helsinki, Finland; [f]Department of Urology, Helsinki University Hospital, Helsinki, Finland; [g]Department of Obstetrics and Gynecology, Helsinki University Hospital and University of Helsinki, Helsinki, Finland

ABSTRACT

Accumulating evidence implicates the microbiome as an important determinant of clinical outcomes in cancer therapies; however, the role of the microbiome in oncolytic virus therapy remains largely unexplored. We investigated the gut microbiome of cancer patients following treatment with the oncolytic adenovirus igrelimogene litadenorepvec (Ad5/3-E2F-d24-hTNF-IRES-hIL2; TILT-123). Baseline fecal samples from phase I clinical trials (NCT04695327 and NCT05271318) were analyzed using shotgun metagenomic sequencing and compared to treatment outcomes. A higher relative abundance of *Alistipes* was observed in patients with treatment benefit, while elevated *Eggerthella* was observed with reduced benefit. These associations were validated in a preclinical mouse model where administration of *Alistipes shahii* improved the efficacy of adenovirus therapy. In addition, enrichment analysis in patient samples showed a positive correlation between higher relative abundance of *Alistipes* and elevated short-chain fatty acids in both feces and serum, which in turn revealed higher circulating neutrophil counts. Finally, in a case study, we observed that adenovirus treatment resulted in increased *Alistipes* relative abundance and reduced *Eggerthella* relative abundance, indicating that adenovirus therapy may beneficially modulate the microbiome. Overall, our findings reveal a novel association between *Alistipes*, *Eggerthella*, and the therapeutic response to oncolytic adenovirus therapy, highlighting their potential as biomarkers or targets for microbiome-based interventions such as pre-, pro-, or postbiotics.

ARTICLE HISTORY
Received 15 October 2025
Revised 25 February 2026
Accepted 30 March 2026

KEYWORDS
Adenovirus; cancer therapy; fecal microbiome; gut microbiome; oncolytic virus therapy

CONTACT Akseli Hemminki akseli.hemminki@helsinki.fi Cancer Gene Therapy Group, Translational Immunology Research Program, University of Helsinki, Helsinki, Finland

Supplemental data for this article can be accessed online at https://doi.org/10.1080/2162402X.2026.2656514.

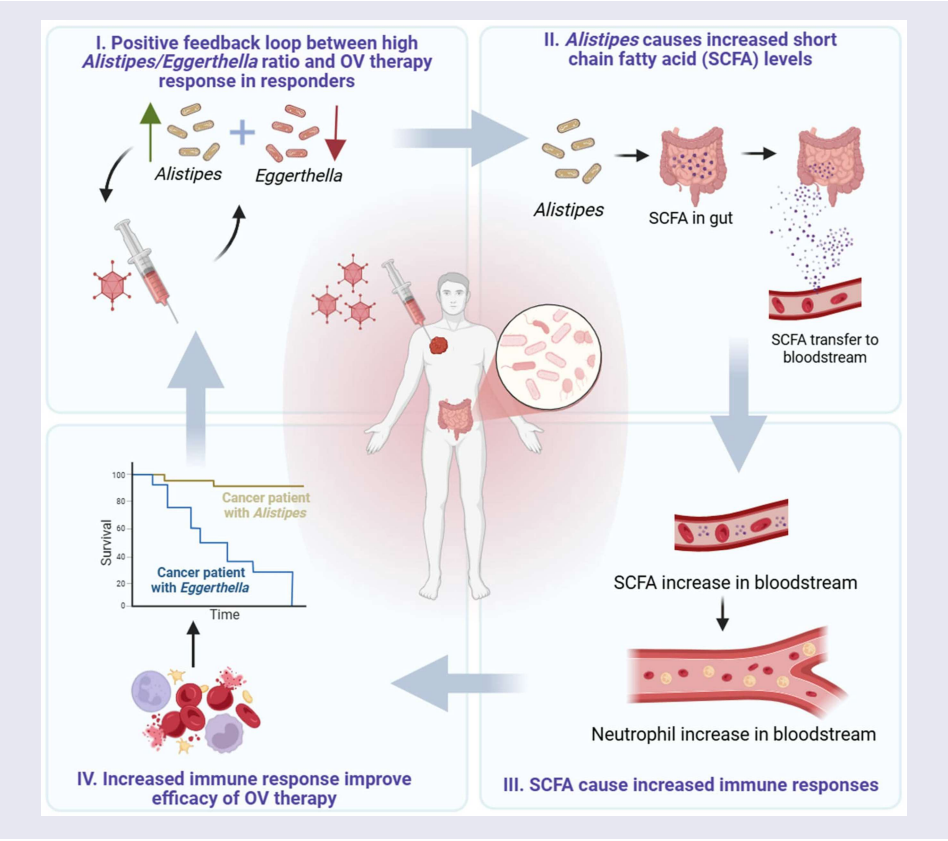

Introduction

Immunotherapies, particularly immune checkpoint inhibitors, have shown promise and received Food and Drug Administration (FDA) and European Medicines Agency (EMA) approvals in several indications; however, their initial success has plateaued; hence, more effective treatment options are needed.[1] In contrast, cancer vaccines and oncolytic viruses have yet to achieve widespread clinical application. Oncolytic viruses, which directly kill tumor cells and trigger a strong anti-tumor immune response, are under active clinical investigation, with several already approved, including T-VEC for metastatic melanoma, H101 for head and neck cancer, and Teserpaturev (DELYTACT®) for glioblastoma.[2]

With the clinical application of immunotherapies, it has become evident that their efficacy is variable and patient dependent. Emerging evidence highlights the microbiome as a key factor influencing therapy outcomes. Notably, studies have shown that alterations in the gut microbiota can affect the response to nivolumab in renal cell carcinoma patients, and studies in advanced-stage non-small cell lung cancer (NSCLC) patients undergoing anti-programmed death protein 1 (aPD-1) therapy identified positive correlations between a higher relative abundance of *Alistipes shahii*, *Alistipes finegoldii,* and *Barnesiella visceriola* in the fecal microbiota and prolonged progression-free survival.[3,4] Additionally, Davar et al. showed that fecal microbiota transplantation (FMT) from aPD-1-responsive donors restored aPD-1 responsiveness in resistant melanoma patients, and Tripodi et al. demonstrated that *Bifidobacterium* spp. supplementation enhanced the antitumoral efficacy of the oncolytic adenovirus Ad5D24-CpG (Ad-CpG) in mice.[5,6]

Given the growing evidence linking the gut microbiome to immunotherapy outcomes, we believe that the microbiome also modulates responses to oncolytic virus therapy. This is supported by pre-clinical findings of Tripodi et al., although clinical validation is lacking.[5] Therefore, we investigated the interaction between the fecal microbiome and oncolytic adenovirus TILT-123, which is currently being evaluated in multiple phase I clinical trials.[7-9] TILT-123 is a human 5/3 chimeric oncolytic adenovirus modified to encode human IL-2 (hIL2) and tumor necrosis factor (TNF) cytokines to enhance T cell recruitment and activation in tumors.[10,11] Understanding the interplay between oncolytic adenoviruses and the microbiome is urgently needed, as the microbiome profile could be used as biomarkers for patient selection or as

therapeutic strategies, where modulation of the microbiome could expand treatment options for patients with otherwise incurable cancers.

Materials and methods

Clinical trials

A total of 8 patients were available after treatment with TILT-123 therapy (Figure 1A, Supp Table S1), including 6 patients in the monotherapy trial TUNIMO, treating advanced solid cancer refractory to standard therapies (TILT-T115, NCT04695327, Figure 1B) and 2 patients in the combination trial PROTA combining adenovirus therapy with pembrolizumab, treating platinum refractory or resistant ovarian cancer (TILT-T563, NCT05271318, Figure 1C).[7,8] TUNIMO trial started 11 January 2021, https://clinicaltrials.gov/study/NCT04695327. The PROTA trial started on 17 May 2022, https://clinicaltrials.gov/study/NCT05271318. Trials are still ongoing, and all participants provided informed written consent prior to enrollment. The inclusion and exclusion criteria have been previously described.[8,9]

Clinical response

Computed tomography (CT) scans were performed at baseline and day 78 in the TUNIMO trial and days 36 and 92 in the PROTA trial of which day 36 was used in this study, as this was the last day before the combination with pembrolizumab started. The treatment response was based on the classification of the Response Evaluation Criteria in Solid Tumors version 1.1 (RECIST1.1). According to RECIST 1.1, treatment response is classified into three categories as measured by CT scans. A partial response (PR) is a $\geq 30\%$ decrease in tumor size. Stable disease (SD) is a $< 30\%$ decrease or $< 20\%$ increase. Progressive disease (PD) is a $\geq 20\%$ increase in tumor size.[12] We grouped patients into disease control (DC), which combines PR and SD patients, as both indicate treatment benefit and no disease control (No_DC), including PD patients.

Patient samples

Fecal samples were obtained on day 1 (TUNIMO, PROTA) and day 36 (PROTA), 16 h (±8h) post-treatment. Samples were stored at −80 °C until use. A complete blood count (with differential), as well as liver and kidney analyses were conducted by routine laboratory testing every visit day pre- and after treatment. The serum was separated from the blood and stored at −20 °C until use. Serum was not available for patient 20211; thus, the patient was excluded from serum-based analyses.

Metagenomics analysis of patient and mice fecal samples

Fecal samples were shipped to Microbiome Insights (Richmond, Canada) for Shallow Shotgun metagenomics sequencing. DNA was extracted using the MagAttract PowerSoil DNA kit (Qiagen) and the libraries were sequenced using llumina Next Seq (2X150 BP), targeting an average of 0.5–2 million reads per sample. Raw reads were pre-processed using the nf-core/taxprofiler [https://github.com/nf-core/taxprofiler; v1.2], including the removal of low-quality reads and host DNA.[13] Cleaned reads were annotated to Greengenes2 and confirmed using MetaPhlan4 databases for taxonomic annotation and to the Humann3 database for functional annotation.[14-16] Downstream analyses were performed via RStudio (4.3.1), following the guidelines in Orchestrating Microbiome Analysis [https://microbiome.github.io/OMA/docs/devel/; v3.21], adjusting for potential confounders, including age and sex (Figure 1D).

Quantification of short-chain fatty acids in patient serum

80 µL of human serum was used with 10 µL of internal standard and 410 µL extraction solvent. The samples were vortexed, centrifuged, and the supernatants were filtered and used for liquid chromatography–mass spectrometry (LC–MS) to determine the short-chain fatty acid (SCFA) concentrations. Analysis was performed at the Helsinki Metabolomics Center, University of Helsinki, Finland.

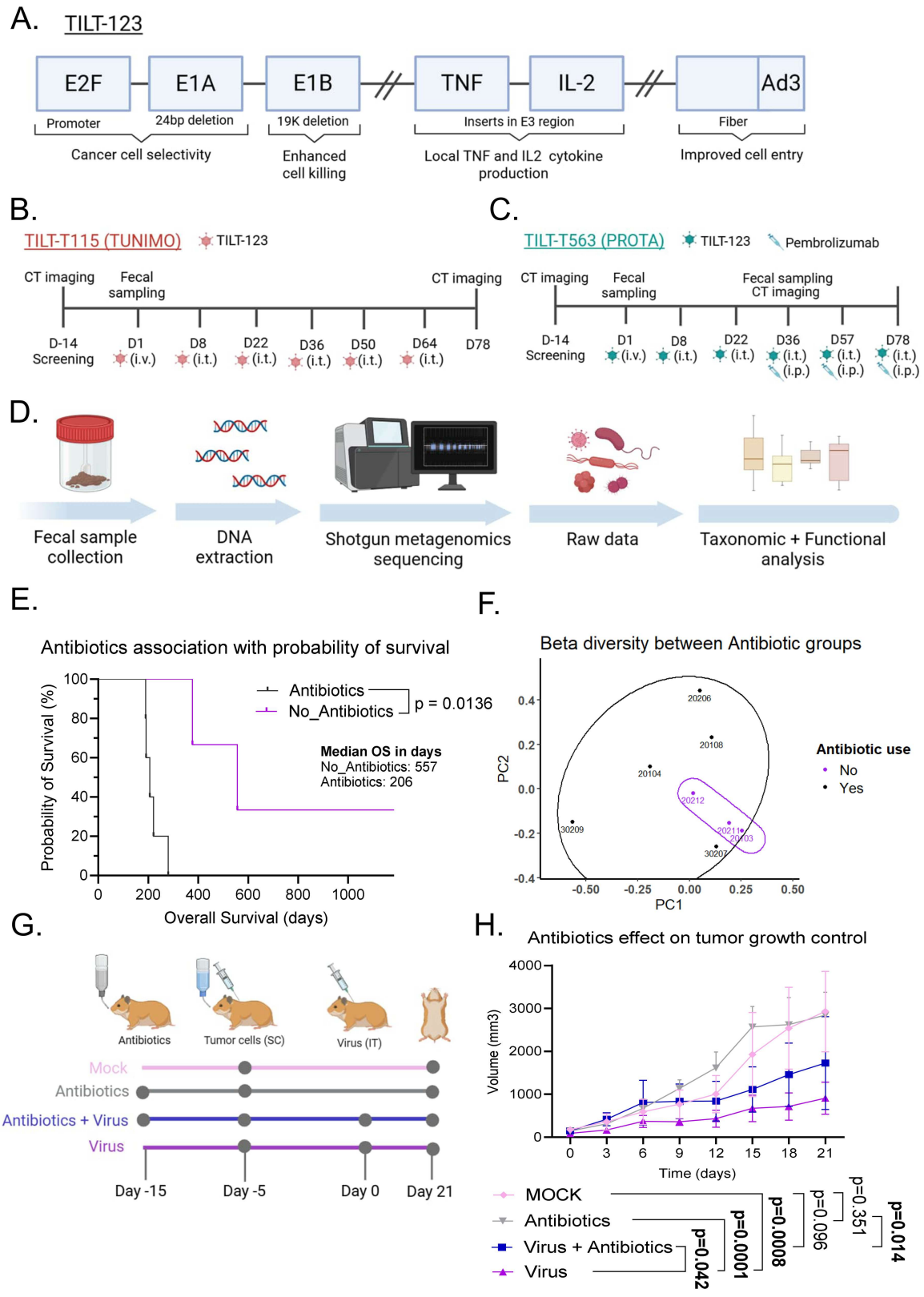

Figure 1. Study design of the fecal microbiota analysis at baseline of TILT-123 therapy. (A) Graphical illustration of the TILT-123 virus used in TILT-123 therapy. (B) Trial outline of the TILT-T115 (TUNIMO) phase I clinical trial. Patients with advanced solid cancer refractory to standard therapies, received one intravenous (i.v.) dose on day 1, followed by intratumoral (i.t.) doses on days 8, 22, 36, 48, and 64 after treatment initiation. (C) Trial outline of the TILT-T563 (PROTA) phase I clinical trial. Patients with refractory ovarian cancer received one i.v. dose on day 1, followed by i.t. doses on days 8, 22, 36, 57, and 78 after treatment initiation. (D) Flowchart of fecal sample analysis. (E) Kaplan–Meier curves for comparing patients who received antibiotics 30 days prior and/or

(*Caption on next page*)

during TILT-123 therapy compared to patients who did not received antibiotics. (F) PCoA based on Bray–Curtis dissimilarity calculated from the species relative abundances. Each point represents an individual sample, colored by antibiotics usage 30 days prior and during TILT-123 therapy. (G) Outline of the animal experiment. Hamsters were engrafted subcutaneously with HapT1 cells and treated with antibiotics in the drinking water to deplete the microbiota. After 10 days, antibiotics treatment was stopped and virus therapy (i.t.) was administered every 3 days. (H) Tumor growth is shown per group, with better tumor growth control in virus-treated animals (purple blue) compared to virus + antibiotic-treated animals (blue) ($P = 0.042$). Statistical analysis for the patient survival curve was done using Mantel–Cox Log-rank test and analysis of tumor growth curve in hamsters using the Kenward–Roger linear mixed model test.

Cell lines & bacterial strains

The Syrian hamster cell line HapT1 (pancreatic ductal adenocarcinoma) was obtained from the Leibniz Institute (DSMZ, Braunschweig, Germany). Murine melanoma cell line B16.OVA was kindly provided by Professor Richard Vile (Mayo Clinic, Rochester, USA). The cells were cultured three times a week prior to engraftment, according to the manufacturer's recommended conditions.

Alistipes shahii WAL 8301 (DSM 19121 #0821, Leibniz Institute, Germany) was grown anaerobically in fastidious anaerobic broth (FAB; Tammer BioLab) at 37 °C for 48 h. Cultures were washed with PBS, pooled, and aliquoted in skim milk for storage at −80 °C.

Eggerthella lenta 1899 B, VPI 0255 (DSM 2243 #0821, Leibniz Institute, Germany) was grown anaerobically on Columbia blood agar plates (CBA; Tammer BioLab) at 37 °C for 48 h. Cultures were collected and stored in skim milk at −80 °C.

For colony forming units (CFU) enumeration, aliquots were pooled, and serial dilutions (1:1–1:1×10^{-10}) were prepared and plated on CBA plates, followed by anaerobic incubation at 37 °C for 48 h.

For animal treatment, bacterial stocks were thawed, centrifuged, washed with PBS, and aliquoted in PBS with 1×10^7 CFU bacteria per 200 µL PBS.

Virus preparation

For the hamster experiment, TILT-123 virus was used. For the mice experiment, a TILT-123 mouse equivalent of cytokine-armed adenoviruses encoding murine IL-2 (Ad5-CMV-mIL2) and TNF (Ad5-CMV-mTNF) was generated as previously described and stored at −80 °C until use.[17] Upon treatment, viral stocks were thawed, resuspended in PBS, and pooled to a total volume of 1×10^9 VP per 100 µL (including a 1:1 ratio of both viruses for the mice study).

Animal experiment

Female five-week-old hamsters were ordered from Janvier Labs, and female six-week-old C57BL/6 mice were ordered from Jackson Laboratory. Hamsters received a cocktail of 1.67 g/l metronidazole and 833.3 mg/l vancomycin for 10 days, while mice received a cocktail of 0.6 g/l ciprofloxacin, 1 g/l metronidazole and 0.5 g/l vancomycin for 9 days in the drinking water. Antibiotics were purchased from Yliopiston Apteekki, Helsinki, Finland. The bottles were changed three times a week. Animals were subcutaneously engrafted with 2×10^6 HapT1 cells (hamsters) or 2.5×10^5 B16.OVA cells (mice). The cells were suspended in 100 µL of RPMI. When the first tumor reached 3–4 mm (mice) or 5–6 mm (hamster) in the longest diameter, animals were randomized and treated three times a week, according to different treatments (Supp Table S2–S4). The viral dosage of 1×10^9 VP was based on previous studies.[5,18] *A. shahii* or *E. lenta* bacteria were i.g. administered using 1×10^7 CFUs, which was a factor of 100 lower compared to previous studies with the same species, to minimize toxic side effects.[19,20] Tumor growth was measured three times a week, and the animals were euthanized via carbon dioxide exposure and cervical dislocation when the Humane endpoint (HEP) was reached (18 mm tumor diameter for mice, 22 mm for hamsters, 20% weight loss, or significant pain symptoms) or when the experiment ended. Tumor volumes were calculated with the formula: (length*width^2)/2, with length defined as the larger dimension. In the mice study, fecal samples were collected per group on day 7. The study adhered to the ARRIVE guidelines.

Flow cytometry

Neutrophils were isolated from whole blood using the MACSxpress® Whole Blood Neutrophil Isolation Kit (Miltenyi Biotec, Germany) and plated 0.5×10^6 cells/well in a 96-well plate, together with 1 mmol/L sodium butyrate (#303410 Merck, Germany), for 2 h at 37 °C. Thereafter, the cells were washed, incubated with Fc Block (#564220, BD Biosciences) and stained with CD11b (#557743, BD Biosciences) and CD66b (#562940, BD Biosciences) for 30 min at 4 °C. Flow cytometry was performed using the Novocyte Quanteon flow cytometer.

Statistics

Statistical analysis was performed using RStudio (4.3.1) or GraphPad Prism (10.1.2). The Wilcoxon test was used to identify taxonomy and predicted pathways. The Wilcoxon test was chosen as a robust non-parametric method that has shown good replicability in recent microbiome benchmarks.[21] The results were confirmed using LinDA test.[22] Due to the small sample size, multiple testing corrections and confounding factors were not included. Instead, *P*-values were used to prioritize the human microbiome data, and animal studies were performed for validation. NetCoMI was used to predict networks.[23] Alpha-diversity used Shannon index. Principal coordinate analysis (PCoA) was based on Bray–Curtis dissimilarity. No statistical test was included for alpha-diversity and beta-diversity. Tumor growth curves included the maximum tumor volume before euthanasia, and statistical analysis was done using the Kenward-Roger linear mixed model test in RStudio. Kaplan–Meier survival curves were generated with GraphPad and analyzed using the Mantel–Cox log-rank test. Correlation curves were analyzed using Pearson correlation when both groups were normally distributed and otherwise using Spearman correlation. Normal distribution was determined using Shapiro-Wilk test ($p > 0.05$ for normal distribution). Flow cytometry was analyzed using unpaired t-test. For graphical illustration, BioRender was used.

Results

Antibiotic use reduces the therapeutic response to oncolytic adenovirus in both patients and animal models

As an initial assessment of the microbiota's influence on the oncolytic adenovirus therapy response, we examined whether antibiotic use prior to and during treatment affected survival outcomes. In this dataset, three patients who did not receive antibiotics before or during therapy had longer median overall survival ($P = 0.014$) as compared to those who did (Figure 1E). No differences were observed in alpha diversity (Supp Figure S1); however, beta diversity analysis suggested that patients who did not receive antibiotics had comparable species-level microbiota profiles, whereas those who received antibiotics showed greater variability, suggesting antibiotic-induced changes in the microbiota (Figure 1F). To confirm the impact of antibiotics, a hamster experiment was performed. Hamsters received antibiotics in their drinking water, after which they were engrafted with tumor cells and treated with TILT-123 adenovirus (Figure 1G). These findings revealed that antibiotic exposure reduced the efficacy of adenovirus therapy in controlling tumor growth (Figure 1H, Supp Figure S2).

Microbiota analysis identifies Alistipes and Eggerthella as key contributors to oncolytic adenovirus therapy outcome

Next, we compared the baseline microbiota profiles between patients who achieved disease control (DC) and those who did not. The microbiota composition between DC patients were comparable (Supp Figure S3). Interestingly, the microbiota profile of patient 20211 (No_DC) resembled that of the DC patients. Notably, this patient exhibited the longest overall survival among all No_DC individuals. We hypothesize that this patient might thus have benefited from therapy despite tumor enlargement on CT, a phenomenon known as inflammatory pseudoprogression.[24]

Given these observations, we hypothesized that specific microbiota compositions may contribute to favorable treatment outcomes. Using the Greengenes2 database, we visualized the most relatively abundant phyla (Supp Figure S4) and genera (Figure 2A) present in DC and No_DC patients,

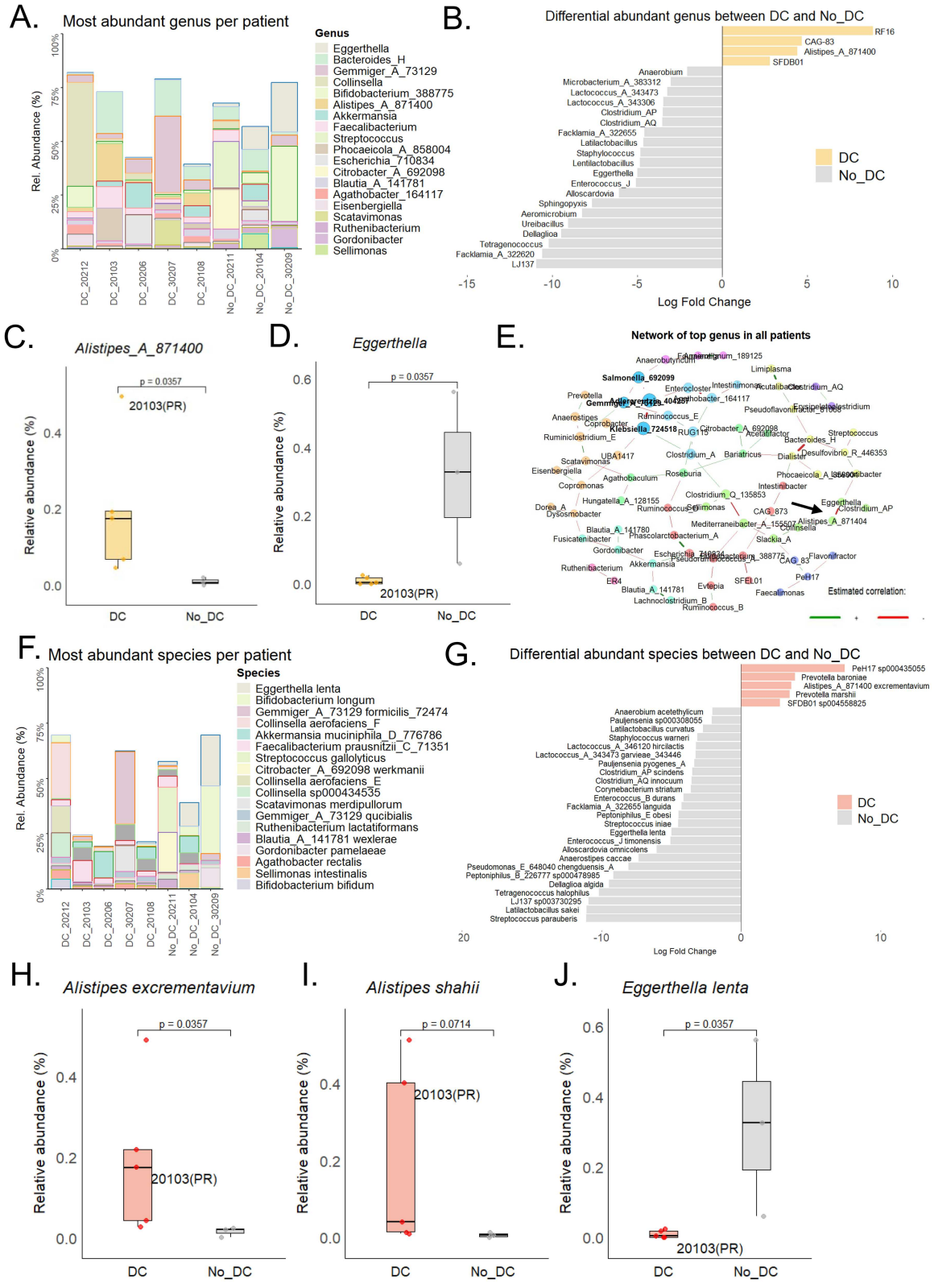

Figure 2. Fecal microbiota differences between DC and No_DC patients. (A) Stacked bar plot including the 12 most relative abundant genera in DC patients and the 12 most relative abundant genera in No_DC patients. (B) Differentially abundant genera between DC and No_DC patients ($P < 0.05$). (C) *Alistipes_A_871400* relative abundance in DC patients compared to No_DC patients ($P = 0.0357$). (D) *Eggerthella* relative abundance in No_DC patients compared to DC patients ($P = 0.0357$). (E) NetCoMi network analysis; the black arrow shows a negative co-abundance relation between *Alistipes* and *Eggerthella*. (F) The 12 most relative abundant species in DC patients and the 12 most relative abundant species in No_DC patients. (G) Differentially abundant species between DC and No_DC patients ($P < 0.05$). (H) *A. excrementavium* relative

(*Caption on next page*)

abundance in DC patients compared to No_DC patients ($P = 0.0357$). (I) *A. shahii* relative abundance in DC patients compared to No_DC patients ($P = 0.0714$). (J) *E. lenta* relative abundance in No_DC patients compared to DC patients ($P = 0.0357$). Statistics were determined using Wilcoxon test. Owing to the small sample size, unadjusted *p*-values were used to prioritize the results.

providing an indication of the microbiota composition of each patient. Additionally, we identified genera that were differentially abundant ($P < 0.05$) between DC patients and No_DC patients at baseline using Wilcoxon test (Figure 2B, Supp Table S5) and LinDA analysis (Supp Figure S5, Supp Table S6). To validate our findings, we repeated the analysis using MetaPhlan4 database, which confirmed solely the different abundances of *Eggerthella* and *Alistipes* genera ($P < 0.05$) between DC and No_DC patients (Supp Figure S6, Supp Table S7). Based on the complementary results from the Greengenes2 and MetaPhlan4 databases, we decided to examine *Alistipes* and *Eggerthella* in greater detail. For *Alistipes_A_71400*, we observed a relatively high relative abundance in the fecal microbiota of DC patients ($P = 0.0357$), with the highest abundance detected in the patient who achieved a partial response (20103) (Figure 2C). Notably, another *Alistipes* sp. strain (*Alistipes_A_871404*) was present in the data, which also showed a relatively high relative abundance in DC patients (Supp Figure S7). In contrast, *Eggerthella* had higher relative abundance in patients with No_DC ($P = 0.0357$) and was completely absent in the partial responder (20103) (Figure 2D). In addition, we conducted a network analysis to visualize the co-abundance variation among the genera. Interestingly, *Eggerthella* genera showed a negative abundance correlation with *Alistipes_A_871404* strain, supporting our previous findings (Figure 2E, Supp Table S8).

Moreover, we examined the microbiota data at the species level, starting with the most relatively abundant species across all patients (Figure 2F), followed by analysis of the species that were differentially abundant ($P < 0.05$) between DC and No_DC patients (Figure 2G, Supp Table S9). These data confirmed our previous findings, which revealed a high abundance of *Alistipes* spp. in DC patients, including *Alistipes excrementavium* ($P = 0.0357$, Figure 2H), but also species not shown in the differential abundance analysis, including *A. shahii* ($P = 0.0714$, Figure 2I). Conversely, *Eggerthella lenta* was more abundant in No_DC patients ($P = 0.0357$), including a zero-abundance observed in the partial responder (Figure 2J).

Alistipes administration improves tumor growth control in mice

Next, we explored the administration of *Eggerthella* sp. and *Alistipes* sp. using a mouse melanoma model. This model was chosen because it has been well-studied for oncolytic adenovirus therapy by our group and others and allows the use of an orthotopic model accessible for intratumoral injections.[5,25] *E. lenta* administration resulted in toxicity in the animals, even though a 100x lower concentration was used compared to previous studies with the same bacteria and mice species.[20] The study of *E. lenta* in animals had to be stopped in accordance with the 3Rs in animal research and our animal permit (Supp Figure S8). For *Alistipes* sp., *A. shahii* was selected because of its commercial availability, it had been previously characterized in murine studies, and it showed high abundance in DC patients.[19] Mice were pre-treated using antibiotics, engrafted with B16.OVA cells and treated three times a week with bacteria followed ~2 h later by virus treatment (Figure 3A). Mice exhibited a transient reduction in body weight following antibiotic treatment; however, they recovered rapidly upon returning to normal water, and no visible adverse side effects were observed (Figure 3B). Individual tumor growth curves are shown (Figure 3C–F). Overall, we observed better tumor growth control ($P = 0.0097$) in the virus + Alistipes combination group as compared to virus therapy alone (Figure 3G). Additionally, fecal pellets were collected from each group for sequencing-based microbiota analysis. Analysis revealed that *Alistipes* spp. was extensively more abundant in the supplemented groups, observed at both genus and species levels (Figure 3H-I). Similar findings were observed in an animal experiment performed without antibiotic pre-treatment (Supp Figure S9). Overall, the findings of these animal studies are consistent with the patient data and suggest that incorporating *Alistipes* sp. into oncolytic adenovirus therapy may improve therapeutic efficacy.

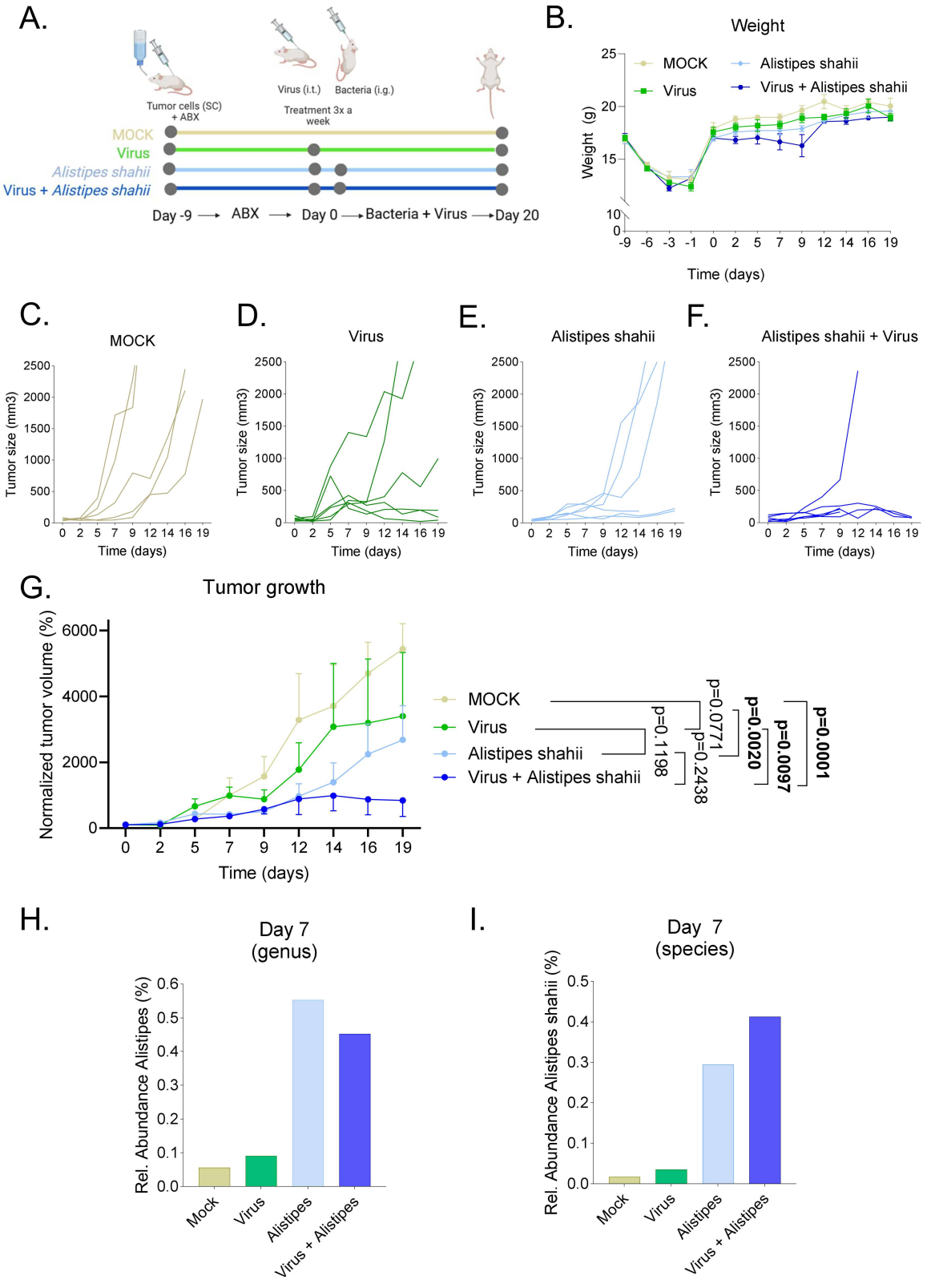

Figure 3. Animal experiment showing the effect of a *A. shahii* WAL 8301 on adenovirus therapy. (A) Outline of the animal experiment. The mice were engrafted subcutaneously with B16.OVA cells and treated with antibiotics in the drinking water to deplete the microbiota. After 9 days, antibiotic treatment was stopped, and *A. shahii* WAL 8301 (i.g.) followed two hours later by virus therapy (i.t.) were administered three times a week until the end of the experiment. (B) Weight curve of the animals during the experiment. (C–F) Individual tumor growth curves for each group. (G) Tumor growth shown per group, including the maximum tumor volume before euthanasia, showing better tumor growth control for

(*Caption on next page*)

virus + Alistipes (dark blue) compared to virus monotherapy (green) ($P = 0.0097$). (H) Relative abundance of the *Alistipes* genus present in the fecal microbiota, as shown per group. (I) Relative abundance of *A. shahii* species present in the fecal microbiota, as shown per group. Tumor growth curve statistics were determined using Kenward–Roger linear mixed model test.

Functional analysis reveals increased short-chain fatty acid activity in patients achieving disease control

Following validation in animals, we proceeded with functional analyses using the patient dataset. Using the KEGG database, we identified several (predicted) pathways that were enriched ($P < 0.05$) between DC and No_DC patients (Figure 4A, Supp Table S10). Firstly, the analysis revealed the upregulation of arginine metabolism pathways in the fecal microbiome of No_DC patients, including the arginine:ornithine antiporter, which is critical for arginine uptake in the gut, and arginine deiminase, which converts L-arginine to citrulline (Figure 4B). Secondly, the increase observed in SCFA transporter activity in No_DC patients ($P = 0.0168$) was of particular interest (Figure 4C). Given that *Alistipes* spp. are known for butyrate production, we hypothesized that the enhanced SCFA transporter activity observed in No_DC patients may represent a compensatory mechanism in response to reduced SCFA availability in the gut. Similarly, we noticed an increase in the acetate coenzyme A (CoA) pathway in No_DC patients ($P = 0.0262$), a pathway that is often upregulated when butyrate levels are low (Figure 4D).[26] Relatedly, we measured enriched levels of butyrate kinase enzymes in DC patients, of which the highest levels were present in the partial responder (Figure 4E). These findings prompted us to examine the relative abundance of other butyrate-producing bacteria, revealing a higher relative abundance of *Faecalibacterium*, *Odoribacter*, and *Coprococcus* in the fecal microbiota of DC patients (Supp Figure S10).

Serum analysis demonstrates a correlation between higher short-chain fatty acid levels and increased neutrophil count

SCFAs are important regulators of the immune response and are known to increase T cells, B cells, and phagocytes.[26,27] Therefore, we investigated whether increased SCFA levels in the fecal microbiome could also be detected systemically. We analyzed patient serum samples for SCFA content and observed higher concentrations of 2-methylvaleric acid in DC patients (Figure 4F) and higher butyric-isobutyric acid and propionic acid concentrations in a subset of DC patients (Figure 4G-H). In addition, we identified correlations between the circulating neutrophil count and the serum concentrations of 2-methylvaleric acid (Figure 4I, $P = 0.043$) and propionic acid (Figure 4J, $P = 0.048$), which was not observed with other measured blood cells. For validation, we conducted an *in vitro* experiment in which neutrophil activation was analyzed upon butyrate exposure. Neutrophils were isolated from whole blood, exposed to sodium butyrate, after which neutrophil activation markers were measured using flow cytometry. This demonstrated that butyrate directly induced neutrophil activation (Supp Figure S11), which has also been shown by others.[28,29] Together, these findings suggest that increases in *Alistipes* abundance in the gut may enhance SCFA production, which can be systemically transported and potentially contribute to elevated neutrophil counts (Figure 4K).

Oncolytic adenovirus administration favorably modulates Alistipes and Eggerthella abundance: a case study

Given that the PROTA trial included fecal sampling at days 1 and 36, we were able to assess the impact of adenovirus therapy on the composition of the fecal microbiome. We investigated DC patient 30207 and No_DC patient 30209 in a case study and observed an increase in *Alistipes* relative abundance upon treatment, with a pronounced rise in the DC patient and a modest increase in the No_DC patient (Figure 5A). Additionally, the relative abundance of *Eggerthella* in the No_DC patient decreased by day 36 compared to day 1 (Figure 5B). At the species level, only modest changes were observed among *Alistipes* spp., including an increase in *A. putredinis* relative abundance in DC patients (Figure 5C) and an increase in *A. communis* in the No_DC patient (Figure 5D).

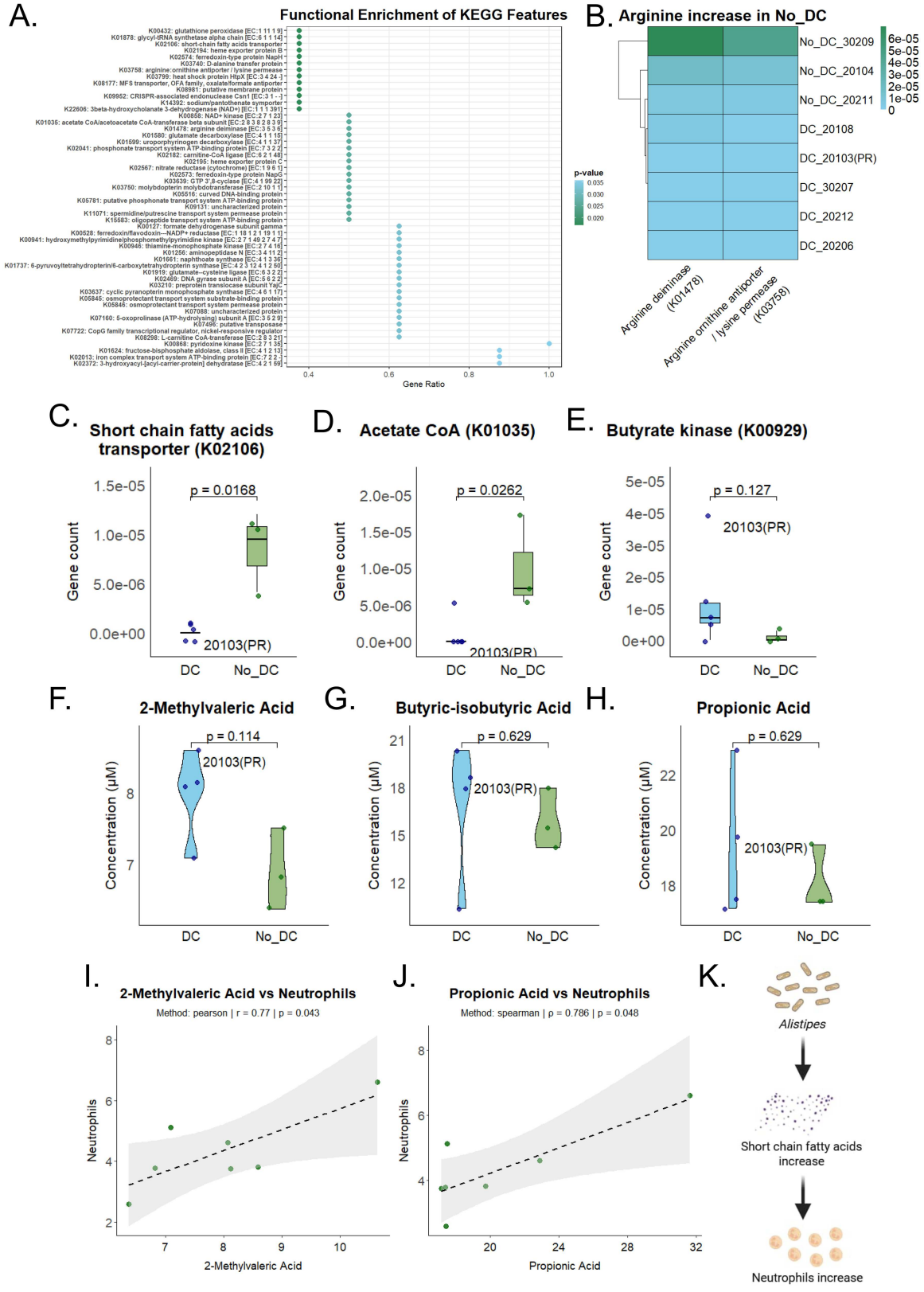

Figure 4. Analysis of the predicted pathways based on the metagenome data. (A) KEGG pathway analysis of the fecal samples showing the most abundant pathways in the fecal samples ($P < 0.05$). Differences are shown between DC and No_DC patients, with color coding representing the *p*-value. (B) Predicted arginine pathway activity in the fecal microbiome, with color coding representing the gene counts. (C) Predicted short-chain fatty acid transporter abundance in the fecal microbiome between DC and No_DC patients ($P = 0.0168$). (D) Predicted acetate CoA abundance in the fecal microbiome between DC and No_DC patients ($P = 0.0262$). (E) Predicted butyrate kinase abundance in the fecal

(*Caption on next page*)

microbiome between DC and No_DC patients ($P = 0.127$). (F) 2-Methylvaleric acid levels in the serum between DC and No_DC patients ($P = 0.114$). (G) Butyric-isobutyric acid levels in the serum between DC and No_DC patients ($P = 0.629$). (H) Propionic acid levels in the serum between DC and No_DC patients ($P = 0.629$). (I) Correlation between 2-methylvaleric acid levels in the serum and neutrophil levels in the blood ($P = 0.043$). (J) Correlation between propionic acid levels in the serum and neutrophil levels in the blood ($P = 0.048$). (K) Graphical summary of *Alistipes* associated with increased SCFA levels in the fecal and blood and increased neutrophil levels in the blood. The KEGG dot plot, boxplot and violin plot statistics were determined using Wilcoxon test. Correlation analysis statistics were determined using Pearson correlation when both groups were normally distributed and otherwise via Spearman correlation (determined using Shapiro-Wilk test, with $p > 0.05$ indicating a normal distribution). Owing to the small sample size, unadjusted *p*-values were used to prioritize the results.

Consistent with the observed shifts in microbial profiles following TILT-123 therapy, supposedly beneficial changes were noted in previously identified activated pathways. These included a complete loss of SCFA transporter activity in the No_DC patient (Figure 5E), a reduced abundance of acetate-CoA ligase activity in the same patient (Figure 5F), and elevated butyrate kinase activity in the DC patient (Figure 5G). Additionally, DC patient exhibited an increased neutrophil count, along with an increase in the proportion of other immune cell types, such as monocytes (Figure 5H). In contrast, similar immune changes were absent in the No_DC patient (Figure 5I), reflecting the smaller increase in the *Alistipes* genus, which may have been insufficient to elicit a systemic effect. Overall, these findings suggest a hypothetical feedback loop in which adenovirus therapy beneficially modulates the microbiome, thereby enhancing the efficacy of the therapy itself (Figure 5J).

Discussion

Emerging evidence suggests that the microbiome is a key determinant of the success of immunotherapy. This study highlights the role of the fecal microbiome in the therapeutic response to oncolytic adenovirus therapy in both humans and rodents. Specifically, we isolated DNA from fecal samples from TILT-123-treated patients, performed shotgun metagenomic sequencing, and pre-processed the data using two independent analysis pipelines that use independent databases (GreenGenes2 and MetaPhlan4) to visualize the bacterial profiles in each sample.[14,15] These profiles were used for downstream processing to compare the most abundant bacteria present in DC and No_DC patients. By using bacterial matrices obtained with two independent pipelines, we minimized the change of false positives. For the downstream analysis, we used the Wilcoxon test and confirmed the results using the LinDA test.[22] This showed that *Alistipes* genera were associated with improved treatment outcomes, whereas *Eggerthella* genera were associated with poor outcomes. Animal studies using *A. shahii* confirmed these findings, although our analysis of human fecal samples suggested that other *Alistipes* spp. likely elicit similar effects. Given that both *Eggerthella* and *Alistipes* include succinate-producing species, we hypothesize that *Eggerthella* spp. and *Alistipes* spp. competes for metabolic niches and influence each other's abundance in the gut.[30,31]

Alistipes are anaerobic gram-negative bacteria within the phylum Bacteroidota, which currently comprises 13 species.[32] *Alistipes* are components of the healthy human microbiota and are most abundantly found in the gastrointestinal tract. Consistent with our findings, increased *Alistipes* spp. abundance has been observed in responders to immunotherapies, including *A. putredinis*, *A. shahii,* and *A. finegoldii* in NSCLC patients and *A. communic* in melanoma patients.[3,33,34] *Eggerthella* are anaerobic gram-positive bacteria within the phylum Actinomycetota, *E. lenta* being the most well-characterized species.[35] While *Eggerthella* is a normal constituent of the healthy gut microbiota, elevated levels have been associated with various pathological conditions, including cancer.[36,37] Consistent with our findings, previous studies demonstrated that a high abundance of *Eggerthella* is associated with poor responses to immunotherapy in NSCLC patients.[38]

Functional analysis showed upregulation of arginine metabolism pathways in patients without disease control. *Eggerthella* is known to use arginine as a substrate for growth; thus, the upregulation of arginine metabolism may have contributed to *Eggerthella* abundance.[39] Additionally, we observed increased SCFA abundance in the fecal and serum samples of patients who achieved disease control. Elevated SCFA levels are likely a consequence of increased *Alistipes* spp. abundance, as members of this genus are well-established SCFA producers.[32,40] SCFAs have been shown to inhibit cancer progression through multiple

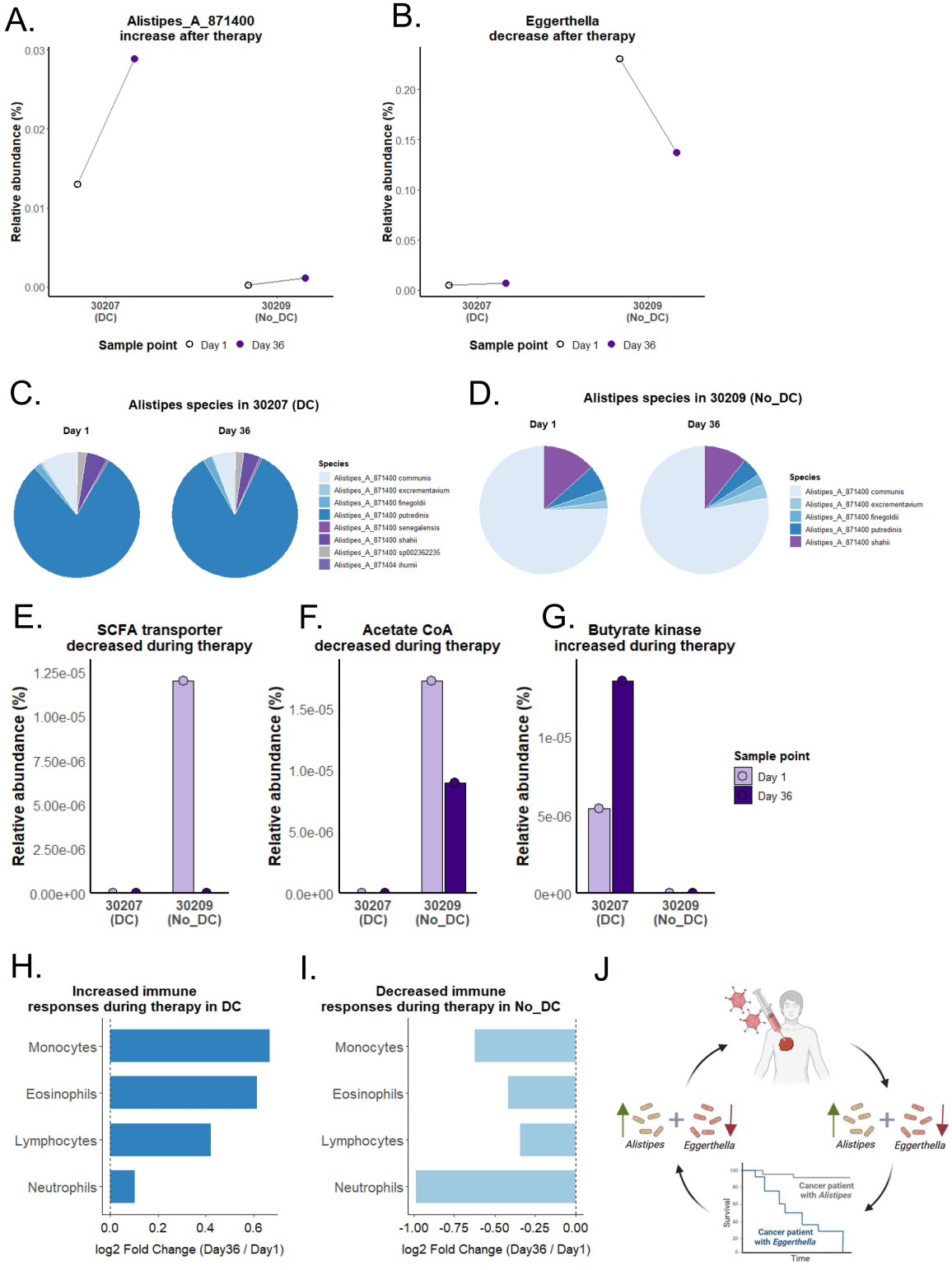

Figure 5. Case study comparing day 1 and day 36 samples from PROTA patients 30207 (DC) and 30209 (No_DC). (A) *Alistipes_A_871400* relative abundance during TILT-123 therapy. (B) *Eggerthella* relative abundance during TILT-123 therapy. (C) *Alistipes* spp. at day 1 and day 36 of TILT-123 therapy in the DC patient. (D) *Alistipes* spp. days 1 and 36 of TILT-123 therapy in the No_DC patient. (E) Predicted SCFA transporter abundance in the fecal microbiome during TILT-123 therapy. (F) Predicted acetate CoA abundance in the fecal microbiome during TILT-123 therapy. (G) Predicted butyrate kinase abundance in the fecal microbiome during TILT-123 therapy. (H) Increased immune cell profiles in the blood of the DC patient upon TILT-123 therapy. (I) Decreased immune cell profiles in the blood of the No_DC patient upon TILT-123 therapy. (J) Proposed graphical summary of a positive feedback loop in which adenovirus therapy affects the microbiota and the microbiota affects the treatment response.

mechanisms and are known to enhance both innate and adaptive immune responses.[27] Interestingly, SCFAs have been shown to promote neutrophil migration, in part, through the induction of the chemoattractant cytokine-induced neutrophil chemoattractant-2αβ (CINC-2αβ) and the upregulation of L-selectin expression on the neutrophil surface, as well as by binding to the G protein-coupled receptor GPR43, which is highly expressed on neutrophils.[29,41] Activated neutrophils secrete pro-inflammatory cytokines such as TNF, which contribute to enhanced antitumor immunity and promote cancer cell death. Notably, TNF is also expressed by TILT-123, underscoring its central role in the findings reported here, where a correlation was observed between elevated SCFA levels, increased neutrophil count, and improved clinical outcomes.

Despite this study being the largest gut microbiome study performed in patients receiving oncolytic virus therapy, a limiting factor in this study is the small sample size, especially in the case study, combined with tumor heterogeneity. As adenovirus therapy is currently still in the clinical trial phase, there is only limited access to fecal samples from adenovirus-treated patients, similar to other cancer microbiome studies.[42-44] Optimally, more fecal samples would be available to confirm and expand upon our data. Another limitation is the use of different animal models. For oncolytic adenovirus therapy, hamster models are preferred because they are permissive to replication of human adenovirus, and they offer a complementary immunocompetent model.[18] However, as intragastric (i.g.) bacterial administration is technically challenging in hamsters, we also used mouse models. C57BL/6 mice were chosen because they have been previously used for *A. shahii* and *E. lenta* administration.[19,20] Mouse models, on the other hand, are not able to replicate adenovirus. Hence, future studies should ideally include different tumor types and including humanized mice or PDX models. Moreover, some levels of toxicity were observed upon *A. shahii* administration. This limitation was addressed by repeating the experiment without antibiotic pre-treatment. Nonetheless, for future animal studies, we suggest performing a pilot to determine the optimal bacterial dose and including groups that directly validate the mechanism of action, such as an adenovirus group treated with SCFAs, or an adenovirus group treated with *A. shahii* in combination with a neutrophil depletion agent. In these studies, tumor and serum samples should be collected for immune cell profiling and SCFA and metabolite analysis. Additionally, more time points should be included for fecal sampling.

Nevertheless, we believe these data are highly valuable, as this is the first microbiome study ever performed on patients treated with oncolytic adenovirus therapy, and our findings offer several translational opportunities for future clinical implementation. First, the identified microbiome signatures could serve as potential biomarkers for patient stratification. Second, our microbiota findings could be used for optimizing donor selection criteria for FMT, as the specific composition and functional traits of a fecal transplant could benefit from further scientific insights.[45] Finally, the findings on the downstream metabolites offer possibilities for advancing into prebiotics, probiotics, and postbiotics research. These agents are currently under extensive investigation for their potential to enhance various cancer therapies.[46,47] However, a clear rationale for selecting the most effective intervention has been lacking.

In summary, this study highlights the role of *Eggerthella* and *Alistipes* in the fecal microbiota, influencing the secretion of SCFA metabolites. SCFAs modulate immune responses essential for effective oncolytic adenovirus therapy. Understanding the interplay between the gut microbiome and oncolytic viruses is vital for enhancing therapeutic response rates and may offer new treatment avenues for patients who currently lack effective options.

Disclosure of potential conflicts of interest

AH, OH, JHAC, DCAQ, LH, VCC, TK, and SKR are employees and shareholders in TILT Biotherapeutics Oy. JMS is a shareholder and was employed at TILT Biotherapeutics Oy at the time of the study. AH is a shareholder in Circio Holdings ASA. PPE has an unrelated research collaboration with Orion Pharma Animal Health.

Acknowledgments

We thank the patients and families enrolled in the trials. Serum analyses were carried out at the FIMM Metabolomics Unit, and flow cytometry was performed at the Biomedicum Flow Cytometry unit, both of which are hosted by the University of Helsinki and supported by HiLIFE and Biocenter Finland. Animal studies were performed at the HiLIFE

Laboratory Animal Center Core Facility, University of Helsinki, Finland. We thank HiLIFe for valuable contribution and support. We acknowledge Microbiome Insights for the shotgun metagenomics sequencing. We thank the Helsinki University Library for supporting open access funding. We thank Minna Oksanen and Sanae Zahraoui for expert assistance.

Author contributions

CRediT: **Mirte van der Heijden:** Conceptualization, Data curation, Formal analysis, Investigation, Methodology, Software, Validation, Visualization, Writing – original draft, Writing – review & editing; **James Hugo Armstrong Clubb:** Conceptualization, Data curation, Formal analysis, Investigation, Methodology, Software, Validation, Visualization, Writing – original draft, Writing – review & editing; **Pande Putu Erawijantari:** Conceptualization, Data curation, Formal analysis, Investigation, Methodology, Software, Validation, Visualization, Writing – review & editing; **Aki Ronkainen:** Conceptualization, Data curation, Formal analysis, Investigation, Methodology, Software, Validation, Visualization, Writing – review & editing; **Victor Arias:** Conceptualization, Data curation, Formal analysis, Investigation, Methodology, Software, Validation, Visualization, Writing – review & editing; **Elise Jirovec:** Conceptualization, Data curation, Formal analysis, Investigation, Methodology, Software, Validation, Visualization, Writing – review & editing; **Tatiana Kudling:** Conceptualization, Formal analysis, Investigation, Methodology, Validation; **Santeri Artturi Pakola:** Conceptualization, Formal analysis, Investigation, Methodology, Validation; **Nea Ojala:** Conceptualization, Formal analysis, Investigation, Methodology, Validation; **Lyna Haybout:** Conceptualization, Formal analysis, Investigation, Methodology, Validation; **Saru Basnet:** Conceptualization, Funding acquisition, Investigation, Methodology, Software, Supervision, Validation, Writing – review & editing; **Susanna Grönberg-Vähä-Koskela:** Project administration, Resources, Supervision; **Sini Karoliina Raatikainen:** Project administration, Resources, Supervision; **Otto Hemminki:** Project administration, Resources, Supervision; **Anna Kanerva:** Project administration, Resources, Supervision; **Dafne Carolina Alves Quixabeira:** Conceptualization, Funding acquisition, Investigation, Methodology, Software, Supervision, Validation, Writing – review & editing; **Victor Cervera-Carrascon:** Conceptualization, Funding acquisition, Investigation, Methodology, Software, Supervision, Validation, Writing – review & editing; **João Manuel dos Santos:** Conceptualization, Funding acquisition, Investigation, Methodology, Software, Supervision, Validation, Writing – review & editing; **Leo Lahti:** Conceptualization, Funding acquisition, Investigation, Methodology, Software, Supervision, Validation, Writing – review & editing; **Akseli Hemminki:** Conceptualization, Funding acquisition, Investigation, Methodology, Software, Supervision, Validation, Writing – original draft, Writing – review & editing.

Funding

This study was supported by iCANDOC Doctoral Education Pilot in Precision Cancer Medicine (PCM, University of Helsinki); Cancer Foundation Finland; Sigrid Juselius Foundation; Jane and Aatos Erkko Foundation; EU Horizon Grant 811693 (UNLEASHAD); Finnish Cultural Foundation; EU Horizon 2020 Research and Innovation Programme under the Marie Skłodowska-Curie Grant Agreement No. 813453; TILT Biotherapeutics Ltd.; HUCH Research Funds; K. Albin Johansson Foundation; Selma and Maja-Lisa Selander's Fund for Research in Odontology; Ida Montin Foundation; Finnish Red Cross Blood Service; Department of Defense. We thank Albert Ehrnrooth and Karl Fazer for their generous research support. Open Access funding was provided by the University of Helsinki.

ORCID

Mirte van der Heijden 0009-0000-4123-6464
James Hugo Armstrong Clubb 0000-0002-9146-4817
Victor Arias 0000-0002-3631-2896
Elise Jirovec 0009-0004-0606-6577
Tatiana Kudling 0000-0003-4481-1617
Santeri Artturi Pakola 0000-0001-6235-8612
Lyna Haybout 0009-0005-5170-5611
Saru Basnet 0000-0003-0268-5982
Dafne Carolina Alves Quixabeira 0000-0003-2614-3942
Victor Cervera-Carrascon 0000-0001-6684-3666

Data availability statement

The data that support the findings of this research are available from the corresponding author, AH, upon reasonable request. Scripts used for analysis are available at [https://github.com/mirteheijden/MicrobiomeProject].

Ethics approval statement

Ethics were reviewed by the Ethical Board of the Helsinki and Uusimaa Hospital District (statement HUS/1804/2020), and the clinical trial protocol was approved by the Finnish Medicines Agency (approval 49/2020). All participants provided informed written consent prior to enrollment. Animal experiments were approved by the Experimental Animal Committee of the University of Helsinki and the Provincial Government of Southern Finland (ESAVI/26562/2022).

Abbreviations

aPD-1	Anti-Programmed Death Protein 1
BP	Base pair
CT	Computed Tomography
DC	Disease Control
No_DC	No Disease Control
PR	Partial Response
CBA	Columbia blood agar
CFU	Colony Forming Units
CINC-2αβ	Chemoattractant Cytokine-Induced neutrophil Chemoattractant-2αβ
CoA	Coenzyme A
DNA	Deoxyribonucleic acid
EMA	European Medicines Agency
FDA	Food and Drug Administration
FAB	Fastidious Anaerobe Broth
HEP	Humane Endpoint
i.g.	Intragastric gavage
i.t	Intratumoral
i.v	Intravenous
KEGG	Kyoto Encyclopedia of Genes and Genomes
LC-MS	Liquid Chromatography Mass spectrometry
NSCLC	Non-Small Cell Lung Cancer
RCC:	Renal Cell Carcinoma
RECIST	Response Evaluation Criteria in Solid Tumors
SCFA	Short-Chain Fatty acid
TNF	Tumor necrosis factor
VP	Viral particles

References

1. Shiravand Y, Khodadadi F, Kashani SMA, Hosseini-Fard SR, Hosseini S, Sadeghirad H, Ladwa R, O'Byrne K, Kulasinghe A. Immune checkpoint inhibitors in cancer therapy. In Current Oncology. 2022;29, pp. 3044–3060 MDPI. doi: 10.3390/curroncol29050247.
2. Gazal S, Gazal S, Kaur P, Bhan A, Olagnier D. Breaking barriers: animal viruses as oncolytic and immunotherapeutic agents for human cancers. Virology. 2024;600:110238. doi: 10.1016/j.virol.2024.110238.
3. Dora D, Ligeti B, Kovacs T, Revisnyei P, Galffy G, Dulka E, Krizsán D, Kalcsevszki R, Megyesfalvi Z, Dome B, et al. Non-small cell lung cancer patients treated with Anti-PD1 immunotherapy show distinct microbial signatures and metabolic pathways according to progression-free survival and PD-L1 status. Oncoimmunology [Internet]. 2023;12(1):1–15. doi: 10.1080/2162402X.2023.2204746.
4. Derosa L, Routy B, Fidelle M, Iebba V, Alla L, Pasolli E, Segata N, Desnoyer A, Pietrantonio F, Ferrere G, et al. Gut bacteria composition drives primary resistance to cancer immunotherapy in renal cell carcinoma patients. Eur Urol. 2020;78(2):195–206. doi: 10.1016/j.eururo.2020.04.044.
5. Tripodi L, Feola S, Granata I, Whalley T, Passariello M, Capasso C, Coluccino L, Vitale M, Scalia G, Gentile L, et al. Bifidobacterium affects antitumor efficacy of oncolytic adenovirus in a mouse model of melanoma. iScience. 2023;26(10):107668. doi: 10.1016/j.isci.2023.107668.
6. Davar D, Dzutsev AK, McCulloch JA, Rodrigues RR, Chauvin JM, Morrison RM, Deblasio RN, Menna C, Ding Q, Pagliano O, et al. Fecal microbiota transplant overcomes resistance to anti-PD-1 therapy in melanoma patients. Science (1979). 2021;371(6529):595–602. doi: 10.1126/science.abf3363.
7. Block MS, Clubb JHA, Mäenpää J, Pakola S, Quixabeira DCA, Kudling T, Jirovec E, Haybout L, van der Heijden M, Zahraoui S, et al. The oncolytic adenovirus TILT-123 with pembrolizumab in platinum resistant or refractory ovarian cancer: the phase 1a PROTA trial. Nat Commun. 2025;16(1):1381. doi: 10.1038/s41467-025-56482-w.

8. Pakola SA, Peltola KJ, Clubb JHA, Jirovec E, Haybout L, Kudling TV, Alanko T, Korpisaari R, Juteau S, Jaakkola M, et al. Safety, Efficacy, and Biological Data of T-Cell-Enabling Oncolytic Adenovirus TILT-123 in Advanced Solid Cancers from the TUNIMO Monotherapy Phase I Trial. Clin Cancer Res. 2024;30(17):3715–3725. doi: 10.1158/1078-0432.CCR-23-3874.
9. Jirovec E, Quixabeira DCA, Clubb JHA, Pakola SA, Kudling T, Arias V, Haybout L, Jalkanen K, Alanko T, Monberg T, et al. Single intravenous administration of oncolytic adenovirus TILT-123 results in systemic tumor transduction and immune response in patients with advanced solid tumors. J Exp Clin Cancer Res. 2024;43(1):297. doi: 10.1186/s13046-024-03219-0.
10. Havunen R, Siurala M, Sorsa S, Grönberg-Vähä-Koskela S, Behr M, Tähtinen S, Santos JM, Karell P, Rusanen J, Nettelbeck DM, et al. Oncolytic adenoviruses armed with tumor necrosis factor alpha and Interleukin-2 enable successful adoptive cell therapy. Mol Ther Oncolytics. 2017;4:77–86. doi: 10.1016/j.omto.2016.12.004.
11. Havunen R, Santos JM, Sorsa S, Rantapero T, Lumen D, Siurala M, Airaksinen AJ, Cervera-Carrascon V, Tähtinen S, Kanerva A, et al. Abscopal effect in non-injected tumors achieved with cytokine-armed oncolytic adenovirus. Mol Ther Oncolytics. 2018;11:109–121. doi: 10.1016/j.omto.2018.10.005.
12. Eisenhauer EA, Therasse P, Bogaerts J, Schwartz LH, Sargent D, Ford R, Dancey J, Arbuck S, Gwyther S, Mooney M, et al. New response evaluation criteria in solid tumours: revised RECIST guideline (version 1.1). Eur J Cancer. 2009;45(2):228–247. doi: 10.1016/j.ejca.2008.10.026.
13. Stamouli S, Beber ME, Normark T, Christensen TA, Andersson-Li L, Borry M, Jamy M, nf-core community, Fellows Yates JA, et al. Nf-core/taxprofiler: highly parallelised and flexible pipeline for metagenomic taxonomic classification and profiling. bioRxiv. 2023. doi: 10.1101/2023.10.20.563221.
14. McDonald D, Jiang Y, Balaban M, Cantrell K, Zhu Q, Gonzalez A, Morton JT, Nicolaou G, Parks DH, Karst SM, et al. Greengenes2 unifies microbial data in a single reference tree. Nat Biotechnol. 2024;42(5):715–718. doi: 10.1038/s41587-023-01845-1.
15. Blanco-Míguez A, Beghini F, Cumbo F, McIver LJ, Thompson KN, Zolfo M, Manghi P, Dubois L, Huang KD, Thomas AM, et al. Extending and improving metagenomic taxonomic profiling with uncharacterized species using MetaPhlAn 4. Nat Biotechnol. 2023;41(11):1633–1644. doi: 10.1038/s41587-023-01688-w.
16. Beghini F, McIver LJ, Blanco-Míguez A, Dubois L, Asnicar F, Maharjan S, Mailyan A, Manghi P, Scholz M, Thomas AM, et al. Integrating taxonomic, functional, and strain-level profiling of diverse microbial communities with bobakery 3. Elife. 2021;10, doi: 10.7554/eLife.65088.
17. Siurala M, Havunen R, Saha D, Lumen D, Airaksinen AJ, Tähtinen S, Cervera-Carrascon V, Bramante S, Parviainen S, Vähä-Koskela M, et al. Adenoviral delivery of tumor necrosis Factor-α and Interleukin-2 enables successful adoptive cell therapy of immunosuppressive melanoma. Molecular Therapy. 2016;24(8):1435–1443. doi: 10.1038/mt.2016.137.
18. Clubb JHA, Kudling TV, Girych M, Haybout L, Pakola S, Hamdan F, Cervera-Carrascon V, Hemmes A, Grönberg-Vähä-Koskela S, Santos JM, et al. Development of a Syrian hamster anti-PD-L1 monoclonal antibody enables oncolytic adenoviral immunotherapy modelling in an immunocompetent virus replication permissive setting. Front Immunol. 2023;14, doi: 10.3389/fimmu.2023.1060540.
19. Lin X, Xu M, Lan R, Hu D, Zhang S, Zhang S, Lu Y, Sun H, Yang J, Liu L, et al. Gut commensal alistipes shahii improves experimental colitis in mice with reduced intestinal epithelial damage and cytokine secretion. mSystems. 2025;10(3), doi: 10.1128/msystems.01607-24.
20. Alexander M, Ang QY, Nayak RR, Bustion AE, Sandy M, Zhang B, Upadhyay V, Pollard KS, Lynch SV, Turnbaugh PJ. Human gut bacterial metabolism drives Th17 activation and colitis. Cell Host Microbe. 2022;30(1):17–30.e9. doi: 10.1016/j.chom.2021.11.001.
21. Pelto J, Auranen K, Kujala JV, Lahti L. Elementary methods provide more replicable results in microbial differential abundance analysis. Briefings in Bioinformatics. 2025;26 10.1093/bib/bbaf130.
22. Zhou H, He K, Chen J, Zhang X. LinDA: linear models for differential abundance analysis of microbiome compositional data. Genome Biol. 2022;23(1):95. doi: 10.1186/s13059-022-02655-5.
23. Peschel S, Müller CL, Von Mutius E, Boulesteix AL, Depner M. NetCoMi: network construction and comparison for microbiome data in R. Briefings in Bioinformatics. 2021;22. doi: 10.1093/bib/bbaa290.
24. Jia W, Gao Q, Han A, Zhu H, Yu J. The potential mechanism, recognition and clinical significance of tumor pseudoprogression after immunotherapy. Cancer Biology and Medicine. 2019;16:655–670. doi: 10.20892/j.issn.2095-3941.2019.0144.
25. Cervera-Carrascon V, Siurala M, Santos JM, Havunen R, Tähtinen S, Karell P, Sorsa S, Kanerva A, Hemminki A. TNFa and IL-2 armed adenoviruses enable complete responses by anti-PD-1 checkpoint blockade. Oncoimmunology. 2018;7(5):e1412902. doi: 10.1080/2162402X.2017.1412902.
26. Mann ER, Lam YK, Uhlig HH. Short-chain fatty acids: linking diet, the microbiome and immunity. Nat Rev Immunol. 2024;24(8):577–595. doi: 10.1038/s41577-024-01014-8.
27. Liu XF, Shao JH, Liao YT, Wang LN, Jia Y, Dong PJ, He D, Li C, Zhang X. Regulation of short-chain fatty acids in the immune system. Front Immunol. 2023;14(May):1–14. doi: 10.3389/fimmu.2023.1186892.
28. Dang AT, Begka C, Pattaroni C, Caley LR, Floto RA, Peckham DG, Marsland BJ. Butyrate regulates neutrophil homeostasis and impairs early antimicrobial activity in the lung. Mucosal Immunol. 2023;16(4):476–485. doi: 10.1016/j.mucimm.2023.05.005.

29. Kamp ME, Shim R, Nicholls AJ, Oliveira AC, Mason LJ, Binge L, Mackay CR, Wong CHY, Sperandio M. G protein-coupled receptor 43 modulates neutrophil recruitment during acute inflammation. PLoS One. 2016;11(9):e0163750. doi: 10.1371/journal.pone.0163750.
30. Wade WG, Dewhirst FE. Eggerthella. In: Bergey's Manual of Systematics of Archaea and Bacteria. Wiley; 2015; p. 1–6. doi: 10.1002/9781118960608.gbm00219.
31. Könönen E, Song Y, Rautio M, Finegold SM. Alistipes. In: Bergey's Manual of Systematics of Archaea and Bacteria. Wiley; 2015; p. 1–7. doi: 10.1002/9781118960608.gbm00251.
32. Parker BJ, Wearsch PA, Veloo ACM, Rodriguez-Palacios A. The genus alistipes: gut bacteria with emerging implications to inflammation, cancer, and mental health. Front Immunol. 2020;11(June):1–15. doi: 10.3389/fimmu.2020.00906.
33. Routy B, Lenehan JG, Miller WH, Jamal R, Messaoudene M, Daisley BA, Hes C, Al KF, Martinez-Gili L, Punčochář M, et al. Fecal microbiota transplantation plus anti-PD-1 immunotherapy in advanced melanoma: a phase I trial. Nat Med. 2023;29(8):2121–2132. doi: 10.1038/s41591-023-02453-x.
34. Jin Y, Dong H, Xia L, Yang Y, Zhu Y, Shen Y, Zheng H, Yao C, Wang Y, Lu S. The diversity of gut microbiome is associated with favorable responses to Anti–Programmed death 1 immunotherapy in Chinese patients with NSCLC. J Thorac Oncol [Internet]. 2019;14(8):1378–1389. doi: 10.1016/j.jtho.2019.04.007.
35. Gardiner BJ, Tai AY, Kotsanas D, Francis MJ, Roberts SA, Ballard SA, Junckerstorff RK, Korman TM, Bourbeau P. Clinical and microbiological characteristics of eggerthella lenta bacteremia. J Clin Microbiol. 2015;53(2):626–635. doi: 10.1128/JCM.02926-14.
36. Woerther PL, Antoun S, Chachaty E, Merad M. Eggerthella lenta bacteremia in solid tumor cancer patients: pathogen or witness of frailty?Anaerobe. 2017;47:70–72. doi: 10.1016/j.anaerobe.2017.04.010.
37. Jiang S, Jianfei E, Wang D, Zou Y, Liu X, Xiao H, E J, Wen Y, Chen Z. Eggerthella lenta bacteremia successfully treated with ceftizoxime: case report and review of the literature. Eur J Med Res. 2021;26(1):1–5. doi: 10.1186/s40001-021-00582-y.
38. Hakozaki T, Richard C, Elkrief A, Hosomi Y, Benlaïfaoui M, Mimpen I, Terrisse S, Derosa L, Zitvogel L, Routy B, et al. The gut microbiome associates with immune checkpoint inhibition outcomes in patients with advanced non-small cell lung cancer. Cancer Immunol Res. 2020;8(10):1243–1250. doi: 10.1158/2326-6066.CIR-20-0196.
39. Albaugh VL, Pinzon-Guzman C, Barbul A. Arginine—Dual roles as an onconutrient and immunonutrient. In Journal of Surgical Oncology. 2017115, pp. 273–280 John Wiley and Sons Inc. doi: 10.1002/jso.24490.
40. Medawar E, Haange SB, Rolle-Kampczyk U, Engelmann B, Dietrich A, Thieleking R, Wiegank C, Fries C, Horstmann A, Villringer A, et al. Gut microbiota link dietary fiber intake and short-chain fatty acid metabolism with eating behavior. Transl Psychiatry. 2021;11(1):500. doi: 10.1038/s41398-021-01620-3.
41. Vinolo MAR, Rodrigues HG, Hatanaka E, Hebeda CB, Farsky SHP, Curi R. Short-chain fatty acids stimulate the migration of neutrophils to inflammatory sites. Clin Sci. 2009;117(9):331–338. doi: 10.1042/CS20080642.
42. Chu CS, Yang CY, Yeh CC, Lin RT, Chen CC, Bai LY, Hung M, Wu C. Endoscopic ultrasound-guided fine-needle biopsy as a tool for studying the intra-tumoral microbiome in pancreatic ductal adenocarcinoma: a pilot study. Sci Rep. 2022;12(1):107. doi: 10.1038/s41598-021-04095-w.
43. Wright RD, Bartelli TF, Baydogan S, White JR, Kim MP, Bhutani MS, McAllister F. Bacterial and fungal characterization of pancreatic adenocarcinoma from endoscopic ultrasound-guided biopsies. Front Immunol. 2023;14, doi: 10.3389/fimmu.2023.1268376.
44. Langheinrich M, Wirtz S, Kneis B, Gittler MM, Tyc O, Schierwagen R, Brunner M, Krautz C, Weber GF, Pilarsky C, et al. Microbiome patterns in matched bile, duodenal, pancreatic tumor tissue, drainage, and stool samples: association with preoperative stenting and postoperative pancreatic fistula development. J Clin Med. 2020;9(9):1–17. doi: 10.3390/jcm9092785.
45. Kang X, Lau HCH, Yu J. Modulating gut microbiome in cancer immunotherapy: harnessing microbes to enhance treatment efficacy. Cell Rep Med. 2024;5(4):101478. doi: 10.1016/j.xcrm.2024.101478.
46. Ciernikova S, Sevcikova A, Drgona L, Mego M. Modulating the gut microbiota by probiotics, prebiotics, postbiotics, and fecal microbiota transplantation: an emerging trend in cancer patient care. Biochim Biophys Acta Rev Cancer. 2023;1878(6):188990. doi: 10.1016/j.bbcan.2023.188990.
47. Miarons M, Roca M, Salvà F. The role of pro-, pre- and symbiotics in cancer: a systematic review. J Clin Pharm Ther. 2021;46(1):50–65. doi: 10.1111/jcpt.13292.